## SUPPLEMENTARY FILE

# A Phase 1 and Pharmacodynamic Study of Chronically-Dosed, Single-Agent Veliparib (ABT-888) in Patients with *BRCA1*- or *BRCA2*-Mutated Cancer; Platinum-Refractory Ovarian or Triple-Negative Breast Cancer

**Julia Manzo[1*], Shannon Puhalla[1,2*], Shalu Pahuja[2], Fei Ding[3], Yan Lin[4], Leonard Appleman[1,2], Hussein Tawbi[1,2], Ronald Stoller[1,2], James J Lee[1,2], Brenda Diergaarde[4], Brian F. Kiesel[1,5], Jing Yu[6], Antoinette R. Tan[7], Chandra P. Belani[8], Helen Chew[9], Agustin A. Garcia[10], Robert J. Morgan[11], Andrea E. Wahner Hendrickson[12], Daniel W. Visscher[13], Rachel M. Hurley[14], Scott H. Kaufmann[12,14], Elizabeth M. Swisher[15], Steffi Oesterreich[16], Tiffany Katz[16], Jiuping Ji[17], Yiping Zhang[17], Ralph E. Parchment[18], Alice Chen[18], Wenrui Duan[19], Vincent Giranda[20], Stacie Peacock Shepherd[20], S. Percy Ivy[21], Edward Chu[1,2], Jan H. Beumer[1,2,5**], ETCTN-8282 study team**

**Address all correspondence to:
Jan H. Beumer, Pharm.D., Ph.D., D.A.B.T.
University of Pittsburgh Cancer Institute
Hillman Research Pavilion, Room G27E
5117 Centre Avenue, Pittsburgh, PA 15213-1863
Tel.: 412-623-3216
Fax: 412-623-1212
Email: beumerj@gmail.com

# METHODS

## Pharmacokinetics

All enrolled patients had blood samples collected for pharmacokinetic (PK) analysis in heparinized tubes prior to and at 0.5, 1, 1.5, 2, 3, 4, 6, 8, and 24 h after veliparib dosing on Cycle 1 Day 1, and Cycle 1 Day 15. There was only a single dose on day 1, whereas from day 2 on, dosing was twice a day. Each blood sample was centrifuged at approximately 1,000 x g, and plasma was stored at -70 °C or colder until analysis. Plasma concentrations of veliparib and M8 were quantitated with an LC-MS assay validated to FDA guidance [15]. Plasma pharmacokinetic parameters were derived from the data by non-compartmental methods with PK Solutions 2.0™ (Summit Research Services, Montrose, CO, USA). Veliparib dose proportionality for day 1 $AUC_{0\text{-}inf}$ and $C_{max}$ was assessed through the power model on log-transformed data as described [55], under the null-hypothesis of dose proportionality. When 1 is not part of the 95%-confidence interval (95%CI) of the coefficient, the null-hypothesis is rejected. Applying the limits for bioequivalence, dose proportionality is only proven when the 90%CI of the coefficient falls completely within the interval of 1+(log(0.8)/log(U/L)) to 1+(log(1.25)/log(U/L)) where H and L are the upper and lower limits of the doses interval studied. Here these calculations result in the interval 0.903 to 1.097. More lenient criterion values have been proposed resulting in an interval of 0.699 to 1.301 [56]. Statistical analyses for pharmacokinetic parameter values were performed using SPSS 23.0 for Windows (SPSS Inc., Chicago, IL).

## Pharmacodynamics

All patients enrolled in the Dose Escalation Phase without a germline *BRCA* mutation as well as patients enrolled in the Dose Expansion Phase were required to have archived tumor tissue available for correlative studies. For patients enrolled in the Dose Escalation Phase with a known *BRCA* mutation, archived tumor specimens were optional.

### γ-H2AX Determination in Tumor Biopsies and Peripheral Blood Samples

Phosphorylated serine-139 (i.e., γ-) H2AX was detected by immunostaining with MAb JBW301 (biotin conjugated, Upstate Biotechnology, then Alexafluor 488 Streptavidin labeling) of formalin-fixed, paraffin embedded biopsies. DAPI counterstaining was performed. The staining protocol was performed on a Vision Biosystems Bondmax instrument, and slides were read on a Nikon microscope with an automated stage and Retiga 2000R CCD camera. Data were collected and analyzed in ImagePro as percent of nuclear area (in the entire field of view) that was positive for γ-H2AX staining. At least 3 fields were imaged per slide, and at least 2 slides per biopsy (from non-overlapping sections of the biopsy) were analyzed. H&E sections were also obtained.

### PAR Immunoassay

PAR concentration was determined by immunoassay. Briefly, 96-well microtiter plates were coated with a monoclonal antibody specific for PAR. After a blocking step, samples were diluted into a buffer and incubated with samples (16 hours at 4˚C). Following a washing step, rabbit antiserum to PAR was added to each well, and an additional 2-hour incubation (at 22˚C) was performed. Another washing step was performed, and a peroxidase-conjugated anti-rabbit antibody was added to each well and incubated for one hour (at 22˚C). Wells were washed again,

a luminol substrate was added, and the assay wells were read in a Tecan Luminometer. A set of calibrators and assay controls set at different PAR levels were run with each assay.

**Methods for Assessment of Cytokeratin 5 and EGFR**

Tumor blocks in patients with unknown *BRCA* mutation status and unknown CK 5 and EGFR status, but known triple-negative status, were assessed for the presence of CK 5 and EGFR by immunohistochemistry. All antibodies were used on the Benchmark XT (Ventana, Tucson, AZ) and developed with iView DAB. The source of antibody to EGFR was Ventana, clone 3C6, using protease 3 conditions and prediluted titers. The antibody to CK 5 was from Cell Marque using clones D5 and 16B4 and CC1 conditions with prediluted titers. Immunohistochemistry slides were semi-quantitated as follows: EGFR was graded as 0, 1+, 2+, 3+. A score of 0 has no staining, 1+ has 10% of cells or less with weak incomplete cell membrane immunostaining, 2+ has at least 10% of cells with complete, weak to moderate cell membrane immunostaining, and 3+ has at least 10% of cells with strong, complete membrane immunostaining. Cytokeratin 5 was scored as positive if invasive neoplastic cells showed any (weak or strong) cytoplasmic or membranous staining.

**Methods for BRCA Protein Expression by IHC**

Paraffin-embedded tissues were cut in 5-μm-thick sections, adhered to silanized slides, deparaffinized, and hydrated by passing through xylene, a graded series of isopropanol, and distilled water. Endogenous perioxidase was blocked with 3% hydrogen peroxide in methanol between the first two steps of washing with isopropanol. After each of the following steps, sections were washed with PBS (pH 7.45) three times for 10 minutes, respectively. Tissues sections were covered in 2% normal rabbit (BRCA1) or swine (BRCA2) serum (DAKO, Glostrup, Denmark) in PBS for 60 minutes, followed by incubation overnight with the primary antibodies detecting BRCA1 (mouse IgG1, clone MS13, diluted 1:20 in PBS; DPC Biermann, Bad Nauheim, Germany) or BRCA2 (clone Ab-2, rabbit polyclonal antibody, diluted 1:50 in PBS; Dianova, Hamberg, Germany). A corresponding section not incubated in antibody served as the control. Antibody specificity was validated further by staining sections with nonimmune isotype serum. To ensure comparability, all samples were stained in parallel for BRCA1 or BRCA2 respectively. Biotinylated rabbit antimouse secondary antibody (BRCA1) or biotinylated swine antirabbit secondary antibody (BRCA2) was added for 45 minutes, and then followed by the avidin-biotinylated peroxidase complex for an additional 45 minutes. Then the slides were washed in PBS for 10 minutes, followed by staining with 3,3'-diamniobenzidine, and then counter-stained with Mayer's hemalaun and mounted.

To analyze these findings, the percentage of cells expressing BRCA 1 or 2 by IHC were determined by assessing the percentage of positively stained nuclei of ductal carcinoma cells in at least 10 high-power fields. The slides were scored as having a labeling index $\geq 50\%$ where $\geq 50\%$ stained positively and was considered positive. Slides where $< 50\%$ of the slides stained positively were considered negative with a labeling index $<50\%$.

**Methods for *BRCA* promoter methylation analysis**

In order to understand whether loss of *BRCA1* expression, as measured by IHC in the clinical samples, was due to previously described epigenetic changes, DNA methylation of the *BRCA1* promoter was studied. The assays analyzed an overlapping portion of the BRCA1 promoter region including 5 CpG sites. This was accomplished through bisulfite pyrosequencing as well as methylation specific PCR (MSP). Briefly, DNA from FFPE samples was isolated, using previously described methods [60]. The DNA was treated with bisulfite (BS) resulting in conversion of

unmethylated C's to T's while methylated C's will remain C's. For the BS conversion, a commercially available kit from Zymo Research was used and the manufacturer's instructions were followed. The pyrosequencing was performed in 96-well plates, using BRCA1 specific primers covering 5 CpG sites in the *BRCA1* promoter using a Pyrosequencer. For pyrosequencing, we used the 75$^{th}$ percentile of the average % methylation (CpG average: the sum of % methylation for the five CpG sites that were evaluated for each sample divided by five) to classify BRCA1 as methylated or unmethylated (≥35.97 is methylated; <35.97 unmethylated). For MSP, DNA was bisulfite converted using EZ DNA Methylation bisulfite conversion kit (Zymo Research). *BRCA1* methylation sensitive PCR was performed in duplicate according to the methods of Esteller et al [61]. In vitro methylated DNA was used as a positive control for bisulfite conversion and MSP. Forty-eight samples were evaluated by pyrosequencing and 43 of those were also assessed by MSP.

**FA triple staining immunofluorescence (FATSI) method using FFPE tissues**.

Fanconi anemia (FA) pathway is a major mechanism of DNA repair related to homologous recombination. FA genes (including BRCA genes) form foci of DNA repair on chromatin after DNA damage or during the S phase of the cell cycle. To evaluate the status of the FA pathway in patient tumors, we developed the Fanconi Anemia triple-stain immunofluorescence (FATSI) assay, which permits the observation (or lack thereof) of FancD2 foci formation in proliferating cells [62]. Briefly FFPE tumor tissue was cut at 4 microns, placed on positively charged slides. One slide was stained with hematoxylin and eosin. Additional two sections for immunofluorescence staining were incubated with a primary antibody cocktail of a FANC-D2 antibody and a Ki67 antibody. The sections were mounted on glass slides using a 4' 6-diamidino-2-phenylindole (DAPI)–containing embedding medium. Formalin fixed paraffin embedded (FFPE) FANCD2 foci positive and negative cells were used as controls on the sample slide during the procedure [62].

**Method for DNA repair protein IHC**

Standard avidin-biotin complex IHC for PARP1, 53BP1 and RAD51 was performed in the Mayo Clinic Pathology Research Core. In brief, after deparaffinization, rehydration and treatment with 0.3% peroxidase, antigen retrieval was performed by steaming the slides for 30 min in EDTA or citrate buffer. The slides were then incubated sequentially with primary antibody, biotinylated secondary antibody, avidin-biotin complex, and chromogenic substrate 3, 3'-diaminobenzidine (DAKO) on a Leica Bond autostainer as recently described in detail [23,57]. The following primary antibodies were used for these studies: anti-PARP1 (1:300, clone E102, Abcam), RAD51 (1:2000, clone EPR4030(3), Abcam), and 53BP1 (mouse monoclonal, a kind gift from Thanos Halazonetis, University of Geneva, Switzerland) diluted in Background Reducing Diluent (Dako) and incubated with slides for 15 minutes. Positive and negative controls included in each staining run consisted of parental HCT116 and a *PARP1*$^{-/-}$ derivative (a kind gift from Eric Hendrickson, University of Minnesota) or parental Ovcar8 cells treated with nontargeting siRNA versus siRNA that knocks down RAD51 or 53BP1 by >90% as confirmed by immunoblotting [23], see also Suppl.Figure 7.

Scoring was performed by two investigators who were blinded to clinical outcome. Intensity of scoring as graded as: 0, negative; 1, weak; 2, moderate and 3, strong. The percentages of tumor nuclei with each intensity were estimated. A modified H-score was calculated as the sum of 1 x % weakly stained nuclei + 2 x % of moderately stained nuclei + 3 x % of strongly stained nuclei, giving a continuous variable from 0-300. Results were displayed as scatter plots.

**Method for tumor biopsies**

Serial tumor biopsies, preferably at least two core biopsy specimens not less than 18 gauge in diameter and at least 1 cm in length, were obtained through Interventional Radiology by a percutaneous approach. All cases were carefully reviewed with the interventional radiologists at participating clinical sites, and if a site was deemed appropriate for biopsy with minimal risk to the participant, an attempt at biopsy was made. The use of imaging (ultrasound, CT scan, or MRI) to facilitate biopsies was decided by members of the Interventional Radiology team. Local anesthesia was administered only if it was considered to be of low risk to the participant. Where possible, one biopsy sample was sent for pathological review and one was sent for correlative studies; if only a single biopsy was feasible, the sample was divided. Upon removal of the biopsy tissue and while still supported in the biopsy needle, the tissue was brought onto a glass slide and cut with a surgical knife into two pieces. Using forceps, each piece was transferred into screw-capped microcentrifuge tubes pre-cooled in liquid nitrogen. The samples were immediately flash-frozen in liquid nitrogen. The tube was transferred into ultra-cold storage at -70˚C. If an initial attempt at percutaneous biopsy was unsuccessful, the patient was given an option to proceed with a repeated attempt at percutaneous biopsy. When biopsy samples were unable to be obtained, the patient remained on study, received study medication, and all other correlative studies were performed. When biopsy attempts were unsuccessful in a particular patient, an additional patient was added to the mandatory biopsy cohort to have a total of 6-12 evaluable patients in whom biopsies were obtained.

# SUPPLEMENTARY TABLES

**Suppl.Table 1. Patient demographics.**

| | *BRCA*mut (n=70) | *BRCA*wt (n=28) |
|---|---|---|
| | Freq. (%) | Freq. (%) |
| Sex | | |
| Female | 65 (93) | 28 (100) |
| Male | 5 (7) | 0 (0) |
| Race | | |
| White | 64 (91) | 21 (75) |
| Black | 3 (4) | 5 (18) |
| Asian | 2 (3) | 2 (7) |
| Native Hawaiian/ Pacific Islander | 1 (1) | |
| Performance status | | |
| 0 | 41 (59) | 18 (64) |
| 1 | 24 (34) | 9 (32) |
| 2 | 5 (7) | 1 (4) |
| Cancer type | | |
| Ovarian | 37 (53) | 4 (14) |
| Breast | 16 (23) | 24 (86) |
| Fallopian tube | 5 (7) | 0 (0) |
| Peritoneal | 4 (6) | 0 (0) |
| Prostate | 3 (4) | 0 (0) |
| Pancreatic | 2 (3) | 0 (0) |
| Endometrium | 1 (1) | 0 (0) |
| Kidney | 1 (1) | 0 (0) |
| Unknown | 1 (1) | 0 (0) |
| Prior treatments | | |
| Median | 5 | 4 |
| Range | 1-19 | 1-9 |

PPC, Primary Peritoneal Cancer

**Suppl.Table 2. Veliparib geometric mean (SD) plasma pharmacokinetic parameters for days 1 and 15 of cycle 1.**

| | D1 | D1 | D1 | D1 | D1 | D1 | D1 | D1 | D15/D1 | D15/D1 |
|---|---|---|---|---|---|---|---|---|---|---|
| Dose (mg, AM) | $C_{max}$ (µg/mL) | $C_{max}$/Dose (ng/mL / mg) | $T_{max}$ (h) | t½ (h) | $AUC_{0-24}$ (µg/mL•h) | $AUC_{0-inf}$[a] (µg/mL•h) | Cl/F (L/h) | $V_{ss}/F$[b] (L) | $C_{max}$[c] ratio | AUC[c] Ratio |
| 50 (N=9) | 0.37 (1.5) | 7.37 (1.54) | 1.5 (2.1) | 6.1 (1.3) | 2.59 (1.44) | 2.77 (1.44) | 18.1 (1.44) | 144 (1.51) | 1.19 (1.53) | 1.37 (1.33) |
| 100 (N=10) | 0.70 (1.6) | 6.99 (1.62) | 1.7 (1.8) | 5.8 (1.2) | 6.12 (1.25) | 6.51 (1.27) | 15.4 (1.27) | 117 (1.26) | 1.29 (1.15) | 1.39 (1.19) |
| 150 (N=11) | 1.28 (1.24) | 8.53 (1.24) | 1.5 (1.8) | 5.8 (1.4) | 8.73 (1.25) | 9.42 (1.32) | 15.9 (1.32) | 121 (1.25) | 1.45 (1.17) | 1.20 (1.12) |
| 200 (N=6) | 1.46 (1.49) | 7.28 (1.49) | 1.1 (1.9) | 6.4 (1.2) | 11.9 (1.56) | 12.8 (1.55) | 15.6 (1.55) | 130 (1.62) | 1.37 (1.25) | 1.57 (1.44) |
| 300 (N=8) | 2.06 (1.11) | 6.87 (1.11) | 1.7 (1.3) | 5.6 (1.4) | 16.5 (1.18) | 17.7 (1.23) | 17.0 (1.23) | 132 (1.24) | 1.31 (1.29) | 1.39 (1.20) |
| 400 (N=16) | 3.69 (1.24) | 9.23 (1.24) | 1.2 (1.8) | 5.9 (1.2) | 25.4 (1.47) | 27.0 (1.50) | 14.8 (1.50) | 110 (1.33) | 1.09 (1.45) | 1.12 (1.31) |
| 500 (N=7) | 3.81 (1.36) | 7.62 (1.363) | 1.5 (1.3) | 5.9 (1.2) | 30.7 (1.53) | 32.9 (1.56) | 15.2 (1.56) | 123 (1.45) | 1.19 (1.55) | 1.31 (1.37) |
| Total (N=67) | - | 7.86 (1.39) | 1.4 (1.8) | 5.9 (1.3) | - | - | 15.9 (1.40) | 123 (1.36) | 1.24 (1.37) | 1.30 (1.29) |

SD, geometric standard deviation.

[a]$AUC_{0-inf}$ extrapolated beyond the last time point sampled was geometric mean 5.1% (range 1.2-25%).

[b]$V_d/F$, overall 135 (1.39) L

[c]Accumulation ratio was calculated as (D1 $AUC_{0-8}$) / (D15 $AUC_{0-8}$) only for subjects receiving the same dose AM and PM. Overall theoretical accumulation ratio based on day 1 half-life was 1.34 (1.12), N=44.

**Suppl.Table 3. M8 geometric mean (SD) plasma pharmacokinetic parameters for days 1 and 15 of cycle 1.**

| | D1 | D1 | D1 | D1 | D1 | D1 | D1 | D1 | D1 | D15/D1 | D15/D1 |
|---|---|---|---|---|---|---|---|---|---|---|---|
| Dose (mg, AM) | $C_{max}$ (µg/mL) | $C_{max}$/Dose (ng/mL / mg) | $T_{max}$ (h) | t½ (h) | $AUC_{0-24}$ (µg/mL•h) | $AUC_{0-inf}$[a] (µg/mL•h) | $AUC_{0-inf}$/Dose (ng/mL•h / mg) | M8/veliparib $C_{max}$ | M8/veliparib $AUC_{0-inf}$ | $C_{max}$[b] ratio | AUC[b] Ratio |
| 50 (N=6) | 0.056 (2.1) | 1.36 (2.16) | 2.9 (1.4) | 7.5 (1.3) | 0.73 (2.1) | 0.84 (2.0) | 16.8 (2.01) | 0.15 (2.6) | 0.30 (2.8) | 1.68 (1.39) | 1.59 (1.42) |
| 100 (N=9) | 0.094 (1.6) | 0.94 (1.6) | 1.9 (1.8) | 8.2 (1.3) | 1.23 (1.62) | 1.45 (1.69) | 14.5 (1.69) | 0.13 (1.9) | 0.22 (1.5) | 1.81 (1.40) | 2.37 (2.00) |
| 150 (N=5) | 0.154 (1.28) | 1.03 (1.28) | 3.4 (1.5) | 6.6 (1.2) | 1.88 (1.32) | 2.09 (1.36) | 13.9 (1.36) | 0.11 (1.3) | 0.22 (1.2) | 1.25 (1.05) | 1.39 (1.08) |
| 200 (N=1) | 0.080 (-) | 0.40 (-) | 4.0 (-) | 13.1 (-) | 1.35 (-) | 1.93 (-) | 9.65 (-) | 0.08 (-) | 0.21 (-) | 1.92 (-) | - (-) |
| 300 (N=4) | 0.199 (1.70) | 0.66 (1.7) | 3.7 (1.8) | 7.4 (1.7) | 2.62 (2.02) | 3.10 (2.35) | 10.4 (2.35) | 0.09 (1.7) | 0.16 (2.2) | 1.56 (1.37) | 1.70 (1.41) |
| 400 (N=11) | 0.382 (1.87) | 0.96 (1.9) | 2.9 (1.7) | 9.5 (1.8) | 4.78 (1.96) | 6.23 (2.13) | 15.6 (2.13) | 0.11 (2.0) | 0.27 (2.0) | 1.38 (1.49) | 1.51 (1.38) |
| 500 (N=7) | 0.321 (1.55) | 0.64 (1.6) | 4.8 (1.2) | 6.5 (1.3) | 3.85 (1.63) | 4.28 (1.68) | 8.56 (1.68) | 0.08 (1.2) | 0.13 (1.5) | 1.35 (1.22) | 1.34 (1.35) |
| Total (N=43) | - | 0.90 (1.8) | 3.3 (1.6) | 7.9 (1.5) | - | - | 13.2 (1.88) | 0.11 (1.8) | 0.21 (1.9) | 1.51 (1.34) | 1.59 (1.41) |

SD, geometric standard deviation.

[a]$AUC_{0-inf}$ extrapolated beyond the last time point sampled was geometric mean 11.6% (range 1.7-53%).

[b]Accumulation ratio was calculated as (D1 $AUC_{0-8}$) / (D15 $AUC_{0-8}$) only for subjects receiving the same dose AM and PM. Overall theoretical accumulation ratio based on day 1 half-life was 1.51 (1.25), N=26.

**Suppl.Table 4. Tumor *BRCA1* promoter methylation status by pyrosequencing and methylation specific PCR.**

| Subject ID | BRCA status | Pyrosequencing % Methylation | | | | | | Pyrosequencing methylation status[a] | MSP methylation status[b] |
|---|---|---|---|---|---|---|---|---|---|
| | | CpG_1 | CpG_2 | CpG_3 | CpG_4 | CpG_5 | Mean | | |
| 1-1-07 | wt | 37.83 | 29.11 | 37.68 | 40.37 | 39.29 | 36.86 | Positive | not done |
| 1-5-27 | mut | 37.73 | 24.12 | 37.21 | 34.46 | 40.57 | 34.82 | Negative | U |
| 1-6-35 | mut | 7.09 | 6.88 | 6.01 | 5.52 | 6.14 | 6.33 | Negative | U |
| 1-7-48 | mut | 22.5 | 14.03 | 22.82 | 24.07 | 20.96 | 20.88 | Negative | U |
| 1-7-51 | wt | 40.86 | 32.48 | 43.08 | 45.76 | 43.18 | 41.07 | Positive | M |
| 1-8-52 | mut | 40.35 | 25.68 | 45.07 | 42.24 | 40.81 | 38.83 | Positive | U |
| 1-8-54 | wt | 23.55 | 14.54 | 20.46 | 26.23 | 26.81 | 22.32 | Negative | U |
| 1-8-61 | mut | 36.82 | 28.12 | 36.02 | 39.06 | 35.03 | 35.01 | Negative | U |
| 1-8-62 | mut | 19.29 | 12.63 | 13.86 | 15.16 | 15.54 | 15.30 | Negative | U |
| 1-8-75 | mut | 13.91 | 8.02 | 12.99 | 12.97 | 11.52 | 11.88 | Negative | U |
| 1-8-76 | mut | 35.95 | 27.91 | 36.2 | 33.6 | 33.87 | 33.51 | Negative | U |
| 1-8-77 | mut | 23.33 | 18.46 | 18.2 | 20.02 | 20.38 | 20.08 | Negative | U |
| 1-8-78 | mut | 52.48 | 41.07 | 43.3 | 49.82 | 51.91 | 47.72 | Positive | U |
| 1-8-82 | mut | 10.78 | 5.9 | 7.96 | 10.7 | 10.14 | 9.10 | Negative | U |
| 1-8-83 | mut | 21.34 | 27.61 | 28.64 | 29.23 | 29.35 | 27.23 | Negative | U |
| 1-8-84 | mut | 16.34 | 11.13 | 16.72 | 15.61 | 13.6 | 14.68 | Negative | U |
| 1-8-85 | mut | 25.66 | 15.19 | 22.69 | 24.31 | 20.81 | 21.73 | Negative | U |
| 1-8-87 | mut | 29.18 | 17.72 | 28.01 | 33.71 | 29.47 | 27.62 | Negative | U |
| 1-8-88 | mut | 25.93 | 14.65 | 22.41 | 23.45 | 25.33 | 22.35 | Negative | U |
| 1-8-94 | mut | 9.51 | 6.03 | 8.17 | 8.72 | 9.56 | 8.40 | Negative | U |
| 1-8-96 | mut | 34.69 | 29.93 | 34.47 | 35.74 | 36.83 | 34.33 | Negative | not done |
| 1-8-98 | mut | 23.6 | 24.58 | 17.71 | 19.48 | 19.13 | 20.90 | Negative | U |
| 1-9-64 | mut | 29.94 | 19.4 | 22.74 | 25.37 | 25.42 | 24.57 | Negative | U |
| 1-9-69 | mut | 36.77 | 27.27 | 31.26 | 37.05 | 35.05 | 33.48 | Negative | M |
| 2-2-15 | mut | 33.31 | 31.27 | 36.47 | 38.04 | 38.13 | 35.44 | Negative | not done |
| 2-5-32 | wt | 28.36 | 26.55 | 32.13 | 28.74 | 29.43 | 29.04 | Negative | M |
| 3-1-03 | wt | 31.18 | 26.8 | 38.36 | 35.84 | 31.03 | 32.64 | Negative | U |
| 3-1-06 | mut | 7.59 | 6.42 | 13.48 | 11.98 | 11.51 | 10.20 | Negative | U |
| 3-1-09 | wt | 37.47 | 35.37 | 45.86 | 38.91 | 41.98 | 39.92 | Positive | M |
| 3-3-20 | wt | 23.1 | 21.37 | 22.5 | 22.89 | 23.83 | 22.74 | Negative | M |
| 3-4-30 | wt | 33.26 | 21.24 | 35.87 | 30.37 | 30.19 | 30.19 | Negative | U |
| 3-8-93 | mut | 37.2 | 42.28 | 42.15 | 44.35 | 47.38 | 42.67 | Positive | U |
| 4-6-40 | mut | 38.77 | 32.54 | 37.32 | 39.15 | 39.04 | 37.36 | Positive | not done |
| 4-8-56 | mut | 31 | 21.92 | 31.15 | 33.79 | 34.39 | 30.45 | Negative | U |
| 4-8-57 | wt | 42.06 | 31.67 | 34.62 | 37.21 | 35 | 36.11 | Positive | M |
| 4-8-59 | mut | 37.77 | 29.01 | 39.42 | 37.71 | 35.96 | 35.97 | Positive | U |
| 4-8-89 | mut | 52.13 | 34.09 | 42.32 | 48.41 | 44.36 | 44.26 | Positive | U |
| 4-8-90 | mut | 31.71 | 20.05 | 26.01 | 26.95 | 24.94 | 25.93 | Negative | U |
| 4-8-95 | mut | 29.83 | 21.66 | 37.39 | 43.07 | 45.62 | 35.51 | Negative | U |
| 4-9-66 | mut | 16.24 | 15.13 | 17.47 | 17.43 | 17.07 | 16.67 | Negative | U |
| 6-2-11 | wt | 37.84 | 24.97 | 21.18 | 39.91 | 15.93 | 27.97 | Negative | U |
| 6-3-17 | mut | 29.08 | 16.41 | 28.13 | 25.83 | 22.51 | 24.39 | Negative | U |
| 6-4-31 | wt | 24.4 | 21.75 | 28.88 | 31.74 | 34.46 | 28.25 | Negative | U |
| 6-5-29 | mut | 50 | 35.28 | 43.41 | 47.33 | 46.06 | 44.42 | Positive | U |
| 6-6-39 | wt | 29.01 | 20.98 | 33.42 | 35.21 | 31.41 | 30.01 | Negative | U |
| 6-7-46 | mut | 23.11 | 32.86 | 29.78 | 26.73 | 23.89 | 27.27 | Negative | U |
| 6-8-58 | wt | 33.32 | 25.81 | 34.19 | 38.04 | 34.93 | 33.26 | Negative | not done |
| 6-8-70 | wt | 34.12 | 32.39 | 36.29 | 38.41 | 39.62 | 36.17 | Positive | U |

[a] *BRCA1* promoter methylation status based on pyrosequencing assay, positive: mean CpG ≥35.97; negative: mean CpG <35.97.

[b] MSP-based *BRCA1* promoter methylation status, U is unmethylated and M is methylated.

# SUPPLEMENTARY FIGURES

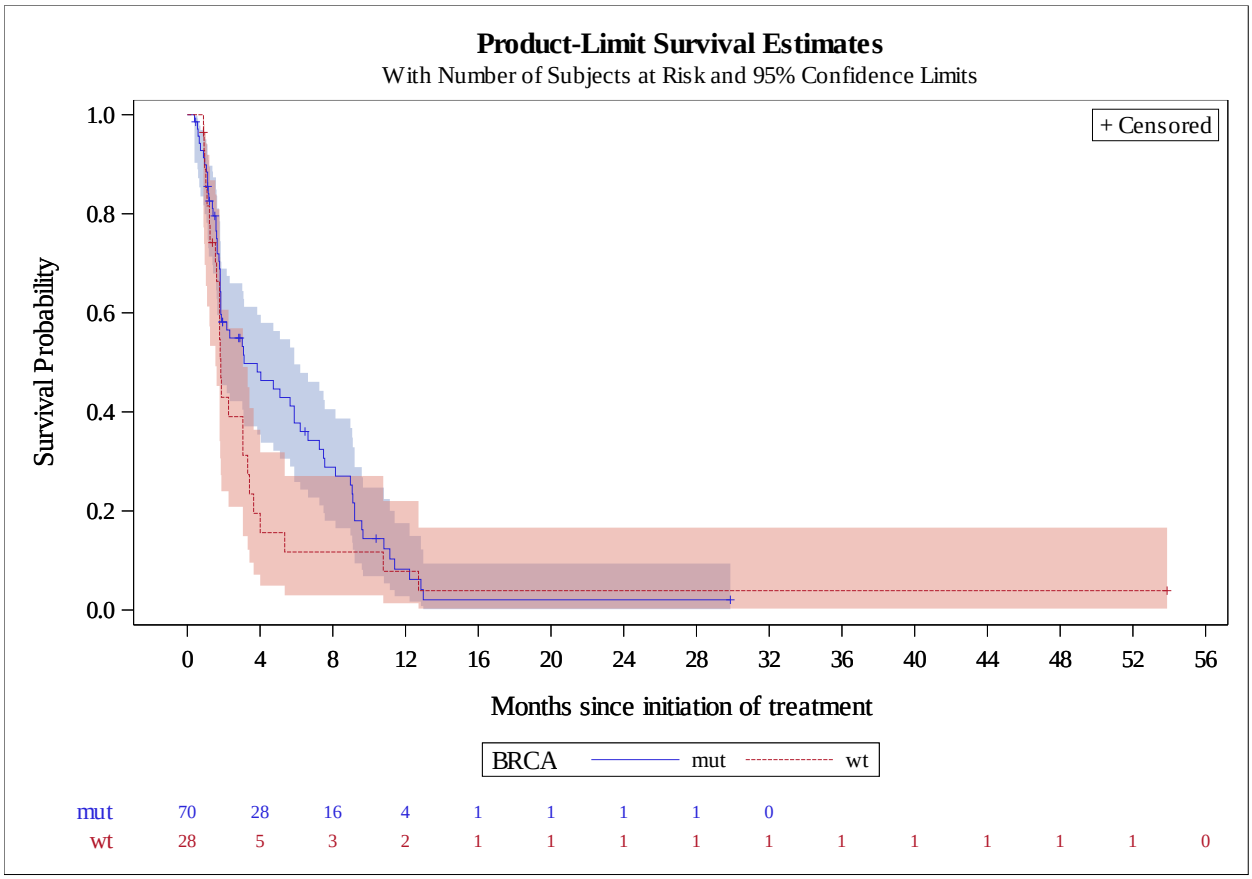


**Suppl.Figure 1. Kaplan-Meier plot of progression-free survival.**

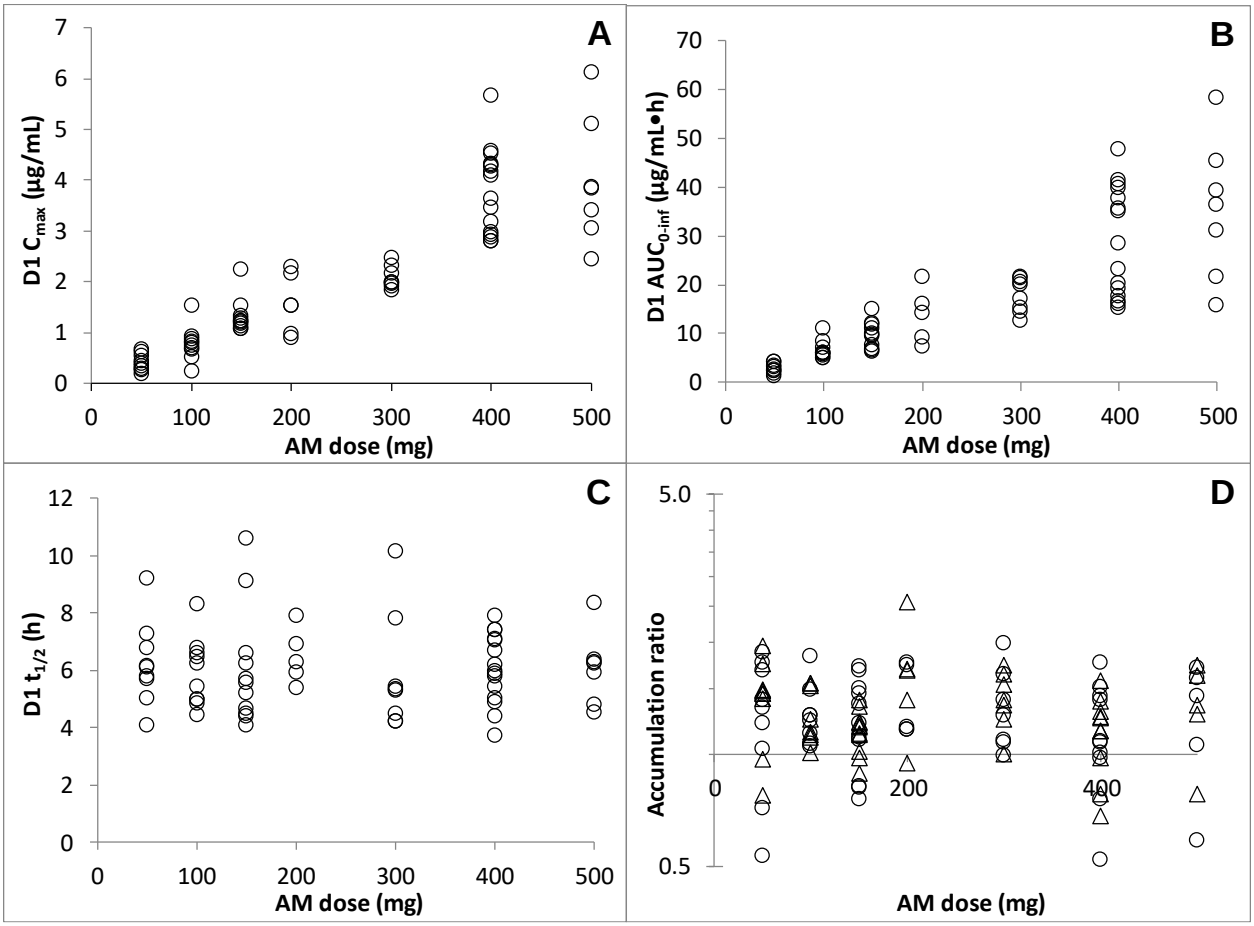


**Suppl.Figure 2. Pharmacokinetic evaluation of veliparib. D1 $C_{max}$ (A), D1 $AUC_{0\text{-}inf}$ (B), D1 $t_{½}$ (C), and accumulation ratio of $C_{max}$ (○) and $AUC_{0\text{-}8}$(Δ) (D), by D1 dose.**

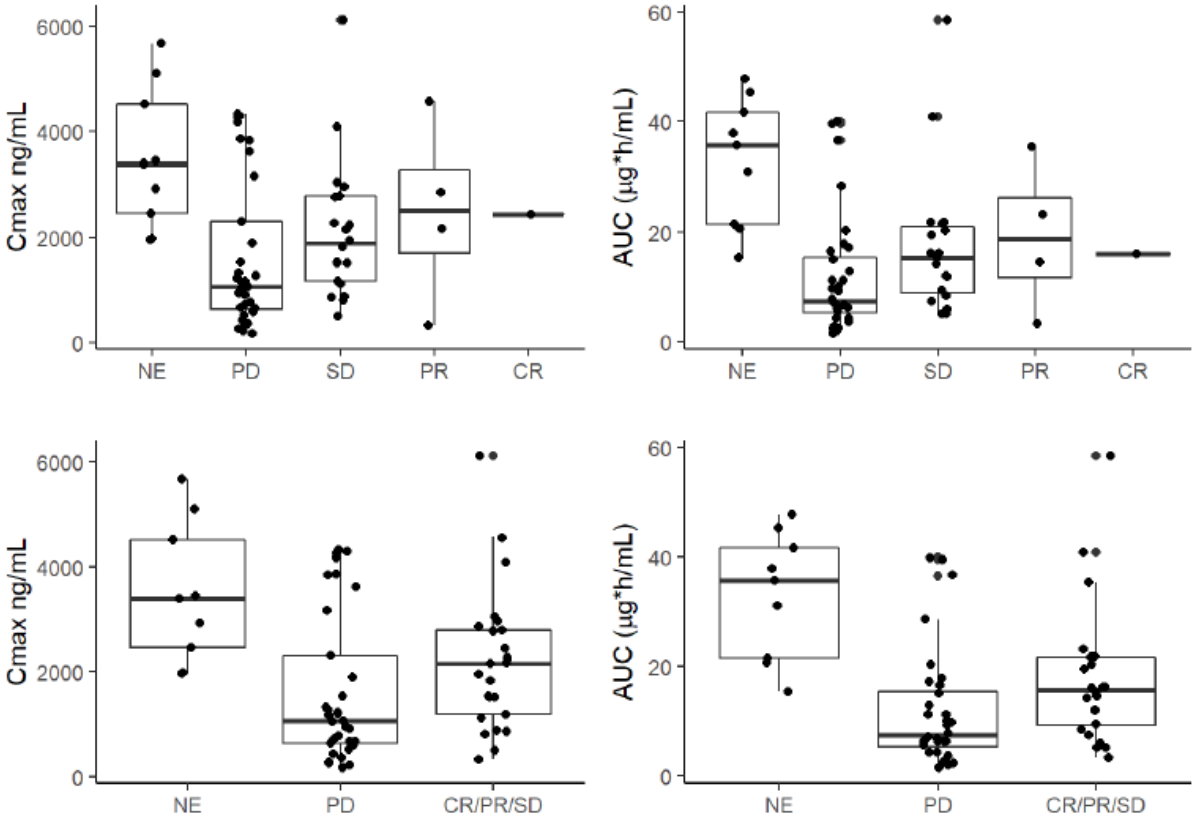


**Suppl.Figure 3. Exposure-response relationship of day 1 veliparib $C_{max}$ and AUC across response categories (top) and (bottom) as progressive disease (PD) vs stable disease (SD), partial response (PR) and complete response (CR) ($C_{max}$ p=0.049, n=58; AUC p=0.019, n=56; per Wilcoxon non-parametric test). Patients not evaluable for response are labelled NE.**

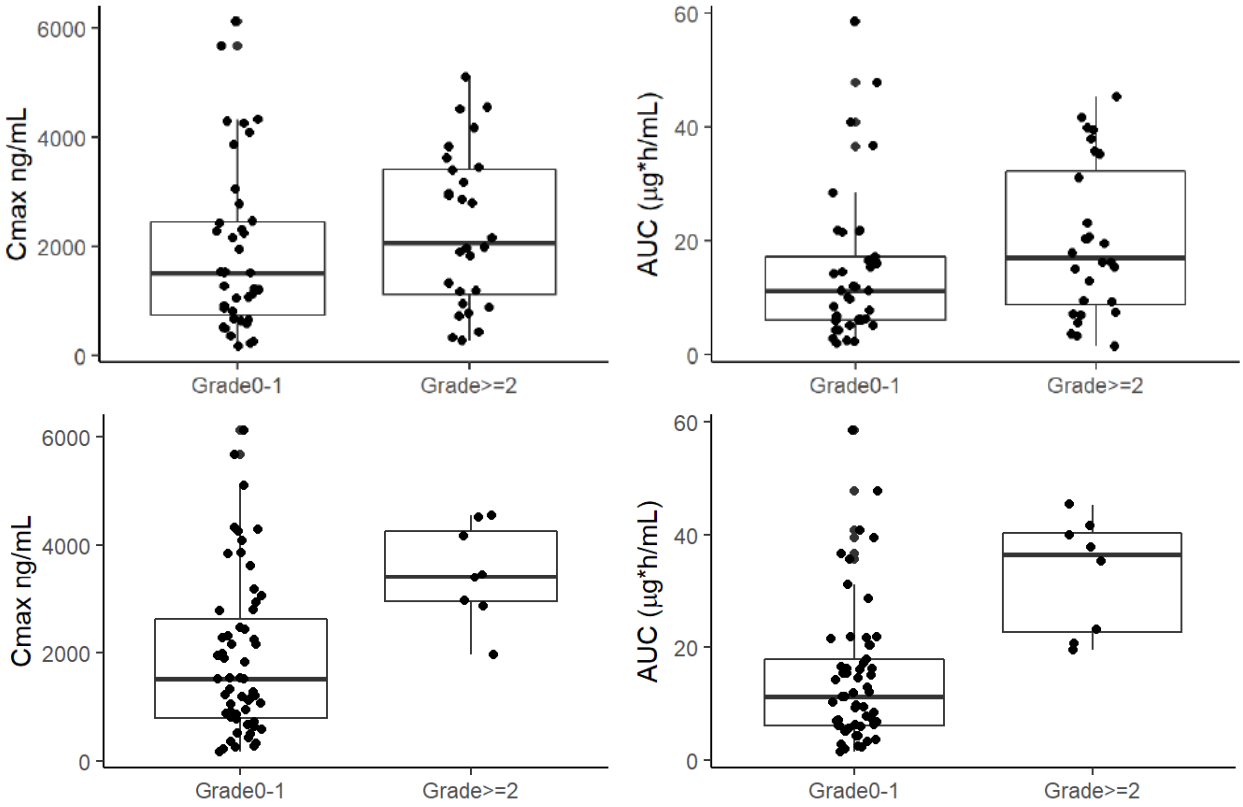


**Suppl.Figure 4. Exposure-toxicity relationship of day 1 veliparib $C_{max}$ and AUC versus: top row, cycle 1 any toxicity grade 0-1 vs grade 2 and up (no significance); and bottom row, cycle 1 nausea grade 0-1 vs grade 2 and up ($C_{max}$ p=0.003, n=67; AUC p=0.0004, n=65; per Wilcoxon non-parametric test).**

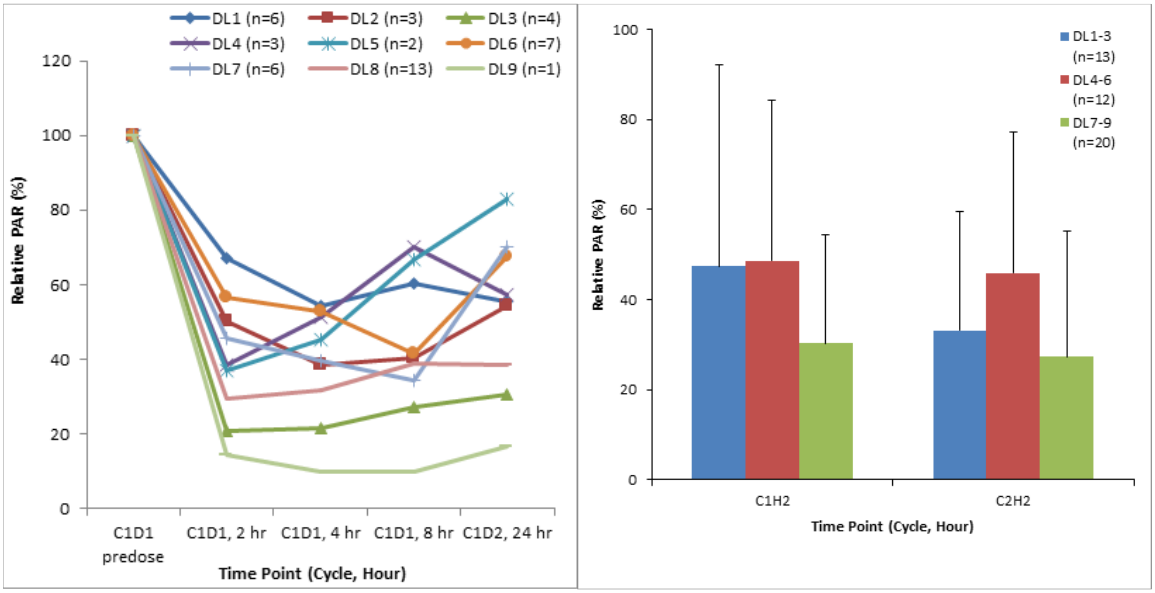


**Suppl.Figure 5. Average relative PBMC PAR levels in patients treated with veliparib by dose level (left), and relative PBMC PAR levels in patients grouped by dose level (right).**

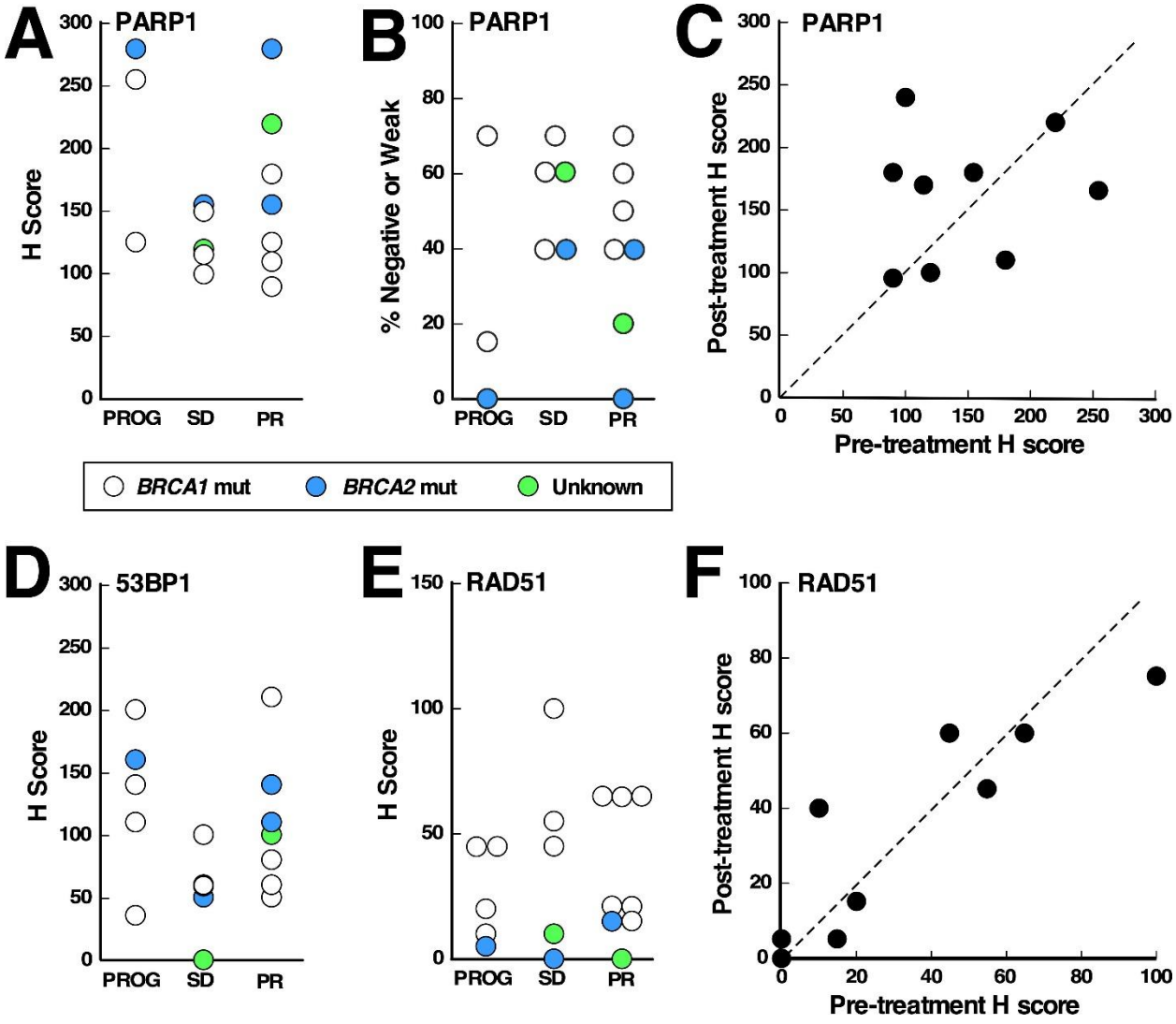


**Suppl.Figure 6. Relationship between response and tumor expression of PARP1, 53BP1 and RAD51. Expression of PARP1, 53BP1 and RAD51 was assessed by immunohistochemistry. A, B, D, E, relationship between response and pretreatment expression of PARP1 (A, B, n = 15), 53BP1 (D, n = 17) and RAD51 (E, n = 17) as summarized by modified H-score (A, D, E) or percentage of tumor nuclei that were weak or negative (B). C, F, relationship between PARP1 (C) or RAD51 (F) H score in initial and post-treatment biopsy. Dashed line indicates values expected if expression did not change.**

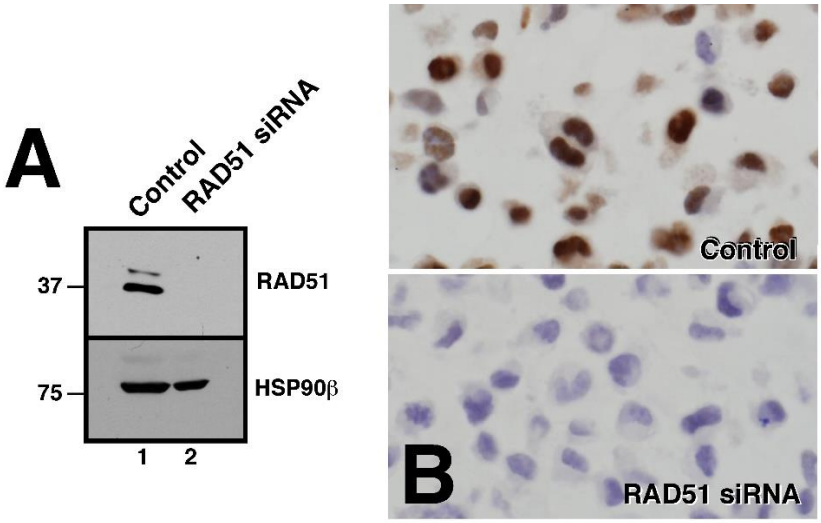


**Suppl.Figure 7. Validation of Rad51 staining. A, immunoblot for Rad51 in Ovcar8 cells transfected with control siRNA (lane 1) or Rad51 siRNA (lane 2). Heat shock protein 90β (HSP90β) served as a loading control. B, aliquots of cells in panel A were formalin fixed, paraffin embedded, and stained with rabbit monoclonal anti-Rad51 (Abcam ab133534) followed by peroxidase coupled secondary antibody.**